Thermal Diode Bridge Applied to Solar Energy Harvesting

By

Zhao, Xiaodong

BS (Southeast University) 2004

A report submitted in partial satisfaction of the
Requirements for the degree of

Masters of Science, Plan II

In

Mechanical Engineering

at the

University of California at Berkeley

Committee in Charge:

_____

Professor Chris Dames, Chair

_____

Professor David Steigmann

Fall 2015

Abstract

Thermal diode bridge applied to solar energy harvesting

By

Zhao, Xiaodong

Master of Science in Mechanical Engineering

University of California, Berkeley

Professor Chris Dames, Chair

The thermal diode bridge is a configuration that can convert *periodical* heating to be *constant*. It is an analogue to the familiar electrical diode bridge in the thermal domain. In this MS report, I first show by modeling that it is possible to use solar energy day-and-night continuously, by exploiting a thermal diode and thermal masses. I next compare my new scheme to the traditional one, which can only work at daytime, and conclude an improvement (in power) of a factor of four in solar energy harvesting. At last, unlike the traditional strategy in solar energy harvesting, which focuses solely on the sun, I also explore an opportunity of a better cold reservoir, outer space, with a typical temperature at 3 K.

Acknowledgement

The author gratefully acknowledges Professor Chris Dames for advising this exciting master's project, and Mitch Westwood, my awesome partner, for doing a perfect job on experimental side. The author also wants to acknowledge Zhen Chen for discussion about model setup, Vivek Mishra for providing information on heat transfer analysis, Geoff Wehmeyer for MATLAB coding and electrical domain suggestion, and Joshua Wilbur for lifting the weight during our lab experiment.

Contents

Chapter 1. Introduction

1-1. Motivation

One of the key limitations for solar energy harvesting is its periodical nature. One may dream to use the hotness of the sun even at nighttime. In this report, we show that this seemingly scientific fiction can actually become true. The magic element to achieve this is a device called thermal diode bridge, a thermal counterpart of the familiar electrical diode bridge, which is used to convert an alternating current (AC) input to a direct current (DC) [1]. We will show how we can use the sun as a hot source and the cold night sky, another important element, as a heat sink to obtain a relatively constant and larger temperature difference to drive a heat engine continuously day and night. Mitch Westwood, my lab mate, experimentally demonstrated this model[2]. The detailed measurement results can be found in his MS project report.

1-2. Concept

From the electrical diode bridge, we can naturally understand the function of a thermal diode bridge: it can help us convert the day-night periodic solar power into a comparably constant thermal power. There are two key parts to make a thermal diode bridge, thermal capacitor and thermal diode. The thermal capacitor, in heat transfer community, is a big amount of the mass. It can be a bulk of metal, a big amount of water, a planet, or even the whole universe. For our modeling, we use materials with high thermal conductivity to ensure the lumped capacity assumption, thus facilitating the thermal analysis. The most famous thermal diode, another key part, which has similar function as electrical diode, was experimentally observed in 1970s[3], and recently re-examined systemically by Dames[4]. Chen and Dames experimentally demonstrated the first photon thermal diode in 2014[5]. With the two parts, making a thermal diode bridge become possible.

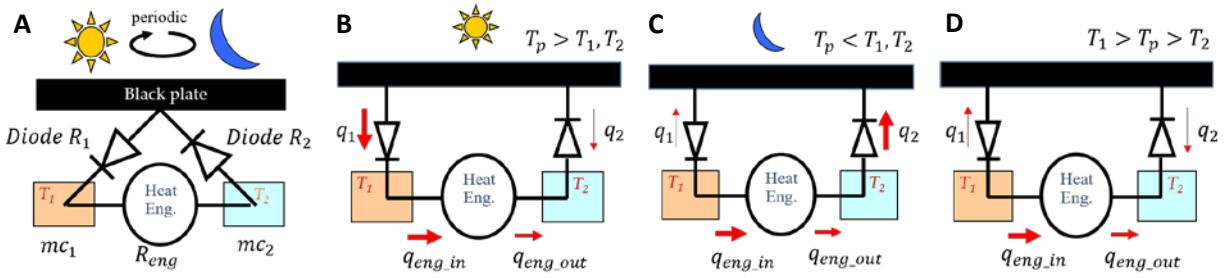

Fig. 1. The configuration of the thermal diode bridge. (A) The basic structure of the thermal diode bridge used for solar energy harvesting. A black plate is used to absorb and transfer the solar thermal to mass one (mc_1) during daytime, and absorb heat from mass 2 (mc_2) and emit to the sky during nighttime. Between two masses is a heat engine with thermal resistance R_{eng} (B) Case one, when $T_p$is higher than both T_1 and T_2, diode one is in forward mode, while diode two is backward mode. We call this case charging section. (C) Case two, T_p is lower than T_1 and T_2, diode one is on backward mode and diode two on forward mode, we call it discharging section. (D) Case three, T_p is lower than T_1 but higher than T_2, both diode are on backward mode.

Our design of thermal diode bridge applied on solar energy harvesting is shown in Fig. 1(A), in which we use a black plate to act with the dual function of a solar absorber at daytime and as an infrared emitter at nighttime. To the back of the plate we attach two thermal diodes, which connect to two thermal masses (mc_1 and mc_2), respectively. A heat engine is driven by the temperature difference of the two thermal masses to convert thermal energy into electrical power. As shown in Fig. 1(B), during daytime, when the plate temperature is higher than both masses, diode 1 is in its forward mode and diode 2 in its backward mode. Mass 1 is thermally charged from the absorber very fast while mass 2 is (nearly) not charged. Similarly, during night time, as shown in Fig. 1(C), when plate temperature is lower than both masses, diode 1 is in backward mode and diode 2 in its forward mode. In this case, mass 2 is discharged to cold sky through the black plate very quickly while mass 1 is (nearly) not discharged. As a result, the temperature of thermal mass 1 goes up faster than that of mass 2 during charging section and the temperature of thermal mass 2 goes down faster than thermal mass 1 during discharging section. During these two sections, the plate temperature is lower than mass 1 but higher than mass 2. The last operating state is when both diodes are in their backward modes, as shown in Fig. 1(D). In this condition none of the masses has much heat exchange with the black plate. However, heat exchange between mass 1 and mass 2 can still drive the heat engine. Eventually, the system will stay periodically stable. In every period, both thermal mass 1 and 2 have (nearly) constant temperatures, and mass 1 is always hotter than mass 2.

Because of the small temperature change for both masses, I finally can get a relatively constant power output because of the relatively constant temperature difference. In this report, I will show that the ripple can be reduced to less than 5%. The ripple here is defined as $0.5\Delta P/P_{avg}$, where ΔP is the difference of maximum power and minimum power, and P_{avg} is the average power over a period of time when it's periodical steady. Since the maximum temperature difference from the sine wave temperature input is $\Delta T_{max} = T_{max} - T_{min}$, and based on the fact that the power output is proportional to ΔT^2[2], I use $P_{max} \propto (\Delta T_{max}^2)$ aas the criterion to evaluate the power output. We define the dimensionless power $P^* = \frac{\Delta T^2}{\Delta T_{max}^2}$. In this report, I show that by using the thermal diode bridge, the power output can reach more than 90% of P_{max}.

Chapter 2. Model setup

2-1 Governing equations for the two masses

Since the temperatures on both sides of the heat engine are the most important thing, I make control volumes of the two masses. The two temperatures are represented by two thermal masses T_1 and T_2. Take the Fig. 1(B) for instance, we can obtain the energy balance equations for the two masses in equation (1a) and (1b). We assume the thermal masses are lumped.

Mass one:
$$q_1 - q_{eng\_in} = mc_1 \frac{dT_1(t)}{dt} \tag{1a}$$

Mass two: $$q_2 + q_{eng\_out} = mc_2 \frac{dT_2(t)}{dt} \quad (1b)$$

q_1 : Heat flow goes to thermal mass 1 through the diode 1

q_2 : Heat flow from thermal mass 2 to diode 2

Notice that when the T_p is higher than T_1 and T_2, both masses gain heat, but q_2 must be much smaller than q_1 since the backward resistance is mucher larger than forward resistance.

mc_1 and mc_2 are the thermal capacitances $[J/K]$ of mass 1 and mass 2, respectively

According to the prescribed temperature input of black plate, T_p (t), which is a function of time, the thermal diode can be in forward or reverse mode. However, once the temperature of the masses are known, the diode's mode is clear. We use R_1 and R_2 to generally describe the thermal resistances of diode 1 and diode 2, use the thermal resistance R_{eng} and efficiency η_{eng} to describe the heat engine.

If we plug all the parameters we defined above into our equations, equation (1a) and (1b) yield to (2a) and (2b)

$$\frac{T_1(t) - T_p(t)}{R_1(T_p, T_1)} + \frac{T_1(t) - T_2(t)}{R_{eng}} = -mc_1 \frac{dT_1(t)}{dt} \quad (2a)$$

$$\frac{T_2(t) - T_p(t)}{R_2(T_p, T_2)} + \left[1 - \eta_{eng}(T_1, T_2)\right] \frac{T_2(t) - T_1(t)}{R_{eng}} = -mc_2 \frac{dT_2(t)}{dt} \quad (2b)$$

Because of the non-linear time dependence, we cannot get a general analytical solution for equation 2a and 2b. The numerical method used to solve the first order ODEs in this report is Euler explicit time-marching method. For a given time step Δt, the approximate temperature value (take equation 2a for example) at next time point can be computed by using the formula:

$$\frac{T_1(i) - T_p(i)}{R_1(i)} + \frac{T_1(i) - T_2(i)}{R_{eng}} = -mc \frac{T_1(i+1) - T_1(i)}{\Delta t}, \quad (3)$$

where *i* indexes the time step.

In order to get accurate solution, the value of Δt is considered. For a 24 hours' time period, $\Delta t = 10[\text{sec}]$ is used. For a model test with time period around one hour, $\Delta t = 0.1[\text{sec}]$ is used. The error of using different time step is checked. Take one hour time period for instance, changing of time step from 0.1[sec] to 10[sec] changes the solution less than 0.002%.

2-2 Two different forms of the black plate boundary conditions

From equation (2a) and (2b), we know that the black plate as the heat source decides the performance. There are two forms of the heat expressions to describe the solar energy,

temperature and heat flux. The temperature profile of most materials put outside is a 24-hour sine wave under engineering approximation[6]. The heat flux measured on earth surface using a blackbody plate face normally to the sunlight is also a half sine wave with a peak at 1000[Wm^{-2}] during the day[7]. In the next two chapters, I will show the analysis by using temperature boundary condition and a more complicated but realistic mix (including solar flux) boundary condition.

Chapter 3. Temperature boundary condition

3-1. Boundary condition analysis

Based on the temperature measurement for different materials from other group[6], we can simplify the input into a sine wave. To decide a 24 hour sine wave temperature in real life, we need to know what the $T_{p\_\max}$ and $T_{p\_\min}$ are.

First, we use sine wave temperature boundary condition as our input. We use a simple black body plate with emissivity equals to one to obtain the maximum and minimum values of sine wave. Because of the atmospheric absorption and scattering, on a clear day, about 27%[8] of the solar input will be reduced before get to the Earth surface, which means the peak solar irradiance reaching the Earth's surface during a day is about 1000[W/m^2][7]. With the energy balance of solar power, convection, and radiation to both the atmosphere and deep space (the cosmos), we obtain the $T_{p\_\max}$ by solving the equation

$$q_{solar\_\max} - h(T_{p\_\max} - T_{amb}) - 0.7\sigma(T_{p\_\max}^4 - T_{atm}^4) - 0.3\sigma(T_{p\_\max}^4 - T_{cos}^4) = 0 \qquad (3a)$$

and $T_{p\_\min}$ by solving

$$h(T_{amb} - T_{p\_\min}) - 0.7\sigma(T_{p\_\min}^4 - T_{atm}^4) - 0.3\sigma(T_{p\_\min}^4 - T_{cos}^4) = 0\,. \qquad (3b)$$

Equations (3) use the following parameters:

$q_{solar\_\max}$ = 1000 [W/m^2] is the maximum solar radiation during a day.

T_{amb} is the ambient temperature, we use the average temperature 17 °C [9] in Oct. 2015 in Berkeley, CA.

T_{atm} is the effective atmosphere temperature. Here I use 255 K which is a calculated average temperature of the troposphere[10], since more than 90% of the atmosphere[10] is in this layer.

$T_{\cos}$ is the cosmos temperature, 2.7 K.

σ is Stefan-Boltzmann constant.

h , 4 $\left[W \cdot m^{-2} K^{-1}\right]$, is the average natural convection coefficient calculated under temperature range from 260 to 400 K, for a square plate with area 1 m^2.

Notice that the radiation heat transfer between the plate and the sky includes two parts. Because of the transparency window of the atmosphere for wavelengths between 8-13μm [11], one part occurs between the plate and the ambient, another part occurs between the plate and the cosmos. If the plate is at temperature around 260-400K, based on the Planck distribution[12], the fraction of radiation over the wavelength 8-13 μm is shown in Table I. For engineering approximation, about 70% of the radiation from the plate emits to the atmosphere and 30% goes to cosmos. By this approximation, if we obtain a temperature of plate out of the range we assumed, we need to use new fraction of radiation to compute more accurate results.

Table I Fraction of blackbody radiation in range 8-13μm under different temperature

Temperature of the blackbody plate[Kelvin]	Fraction of radiation in range 8-13 μm
260	29%
300	32%
400	34%

3-1. Numerical solutions

From the previous analysis, we obtained the maximum and minimum temperatures are 356K and 264K, respectively. For convenience, I chose $T_p = 315\ K + (45\ K)\sin(\omega t)$ as my temperature boundary condition.

For any specific heat engine and thermal diode, we know the thermal resistance R_{eng} and thermal resistances of forward diode R_f and backward diodeR_b. If we give a mass size, we are able to solve the coupled equation (2a) and (2b). Table II shows the original setting of parameters used in getting the numerical solutions.

Table II. Parameters used for baseline calculations of Fig.2

Parameter	Value	Parameter	Value
R_{eng}	3.5 K/W	mc_1	12,000 J/K
R_f	(1/20) R_{eng}	mc_2	12,000 J/K
R_b	20 R_{eng}	Time period, τ	2 hours

The numerical solution of T_1 and T_2 is shown in Fig. 2. As we expect, the upper plot of Fig.2A clearly shows that the temperatures of T_1 and T_2 become periodical steady after several periods. Figure 1B is the temperature profile after periodical steady, for every period, a charging phase of the hot mass and a discharging phase of the cold mass can be observed. From section 1-2, we know that the power output is proportional to ΔT^2, so the fraction of $\Delta T^2/\Delta T_{max}^2$ is the scaled power output. The lower plot of Fig.2A shows that based on the parameters from Table II, the scaled power output is about 40%.

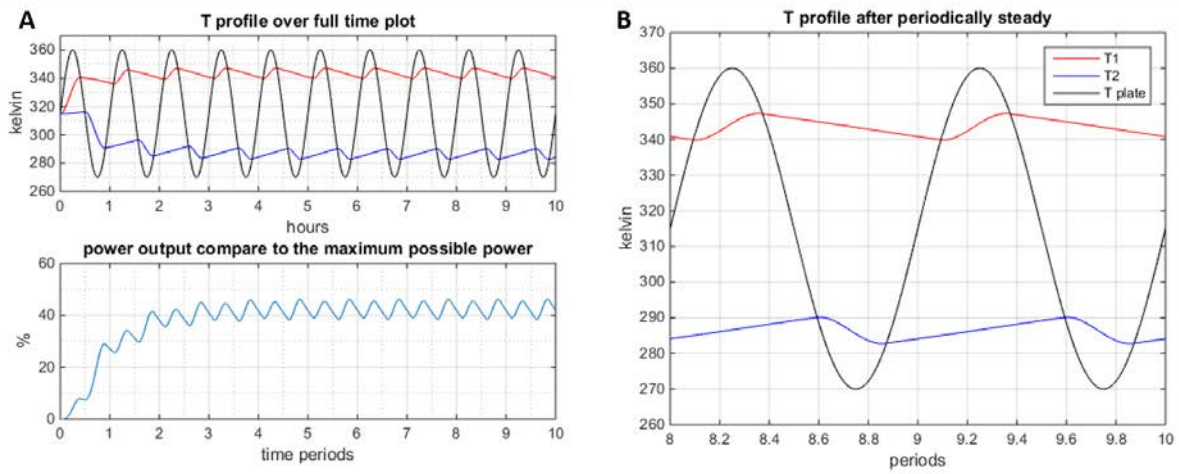

Fig. 2 The numerical solutions of T_1 and T_2 for the baseline scenario. (A,top) is the temperature profiles over 10 time periods. Red line is T_1, blue line is T_2, and black line is temperature of plate T_p. After about three periods, the system becomes steady periodic. (A,bottom) is the power output performance. Based on the parameters I use, the power output is about 40% of the maximum possible power. (B) is the temperature profile after periodic steady. The increasing part of the $T_1$is the charging phase of hot mass. Likewise, the decreasing part of T_2 is the discharging phaseof cold mass.

As can be seen in Fig.2B, the T_1 and T_2 still have room to improve. We expect to obtain a higher T_1 and a lower T_2 by adjusting the thermal capacitor (mass size) and thermal diode(forward and backward resistance). In the next section, I will show how the themal capacitor and thermal diode change the power output.

3-2. Optimization

In order to optimize the thermal diode bridge system, different thermal capacitors (mass size) and different thermal diodes (forward and backward thermal resistance) are tested. The results are shown in Fig.3. As can been seen from Fig.3A, a larger mcR_{eng}/τ gives larger power. Here mc is the mass size for both mass 1 and mass 2, for convenience. The dimensionless group mcR_{eng}/τ is called the dimensionless time constant of R_{eng}. From Fig.3B, we can see that use R_{eng}as criterion, a scaled small R_f gives more power output, but the effect of scaled R_b is relatively small The optimization process will be discussed in 3-2-1 and 3-2-2.

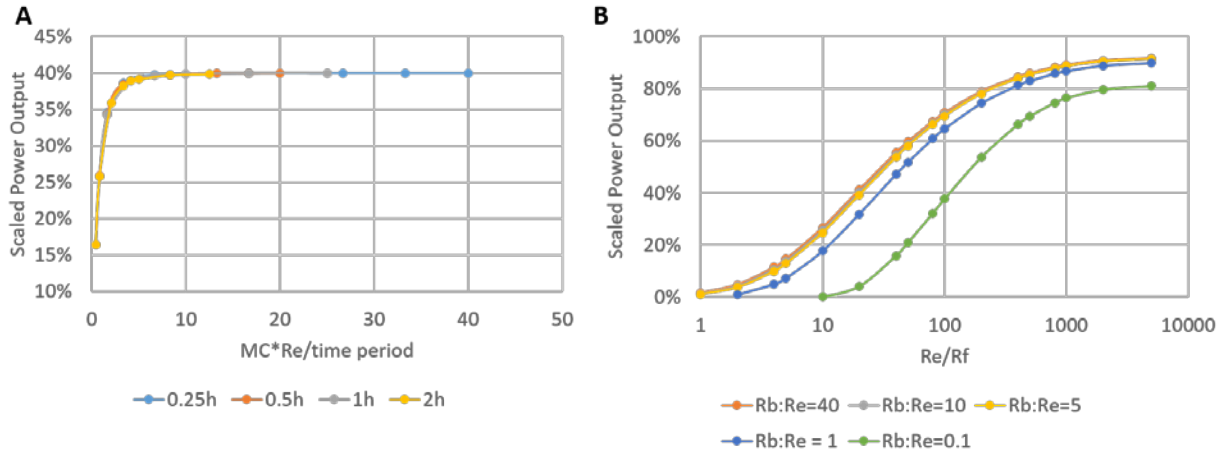

Fig. 3 The optimization of the thermal capacitor and thermal diode. (A) is the power and dimensionless time constant plot. R_f is set to be $R_{eng}/20$ and R_b is set to be $20R_{eng}$. The X-axis is the dimensionless time constant. Four different time periods(0.25 hour, 0.5 hour, 1hour and 2 hours) are tested and they all merge together when the dimensionless time constant is used as x-axis. (A) shows that up until a certain value, the larger time constant gives larger power output. However there is a capped power output no matter how big the dimensionless time constant $\mathrm{mc}R_{eng}/\tau$ is (B) is the power-diode resistance plot. The dimensionless time constant (corresponding to the mass size) is set to be 40. X-axis is the ratio of heat engine resistance to diode forward thermal resistance. The large value means small forward resistance, and gives more power output. For the backward resistance effect, only when backward diode resistance is smaller than heat engine resistance, can the change of power output be detected.

3-2-1 Optimization of thermal mass size.

To optimize for best steady-periodic performance, we first fix the thermal diode resistance as $R_f = 1/20R_{eng}$ and $R_b = 20R_{eng}$ but change the mass size (assuming matched masses: $mc_1 = mc_2 = mc$). As shown in Fig. 3A, I conclude that the larger the mass is, the more power output (corresponding to the square of temperature difference of T_1 and T_2) I can get. However, when the thermal mass becomes very large, the power output doesn't change anymore. I tested four different time periods, $\tau = 2\pi/\omega$ =0.25 hour, 0.5 hour, 1 hour and 2 hours, respectively. In all cases the power outputs converge to a certain value P_m. Such evidences prove that with large thermal mass we can get high power output, however, there is an upper limit under certain values of R_f and R_b, no matter how big the mass is.

To observe the relation of the time period and the mass size, I make a dimensionless group mcR_{eng}/τ as the x-axis, where τ is the time period. We call mcR_{eng}/τ the dimensionless time constant of heat engine. The outputs under different time periods merge together, as shown in Fig. 3A. From Fig. 3A, we conclude that in order to get a good performance, a large time constant is needed. However, for economical and design reason, a small mass might more reasonable. As can be seen, when the dimensionless time constant is larger than 10, the power output barely changes. If the power output under mcR_{eng}/τ =20 is set to be 1, by our calculation, mcR_{eng}/τ =8 still provides about 0.994 power. Some comparisons based on the

dimensionless time constant is shown in Table III. For modeling, a dimensionless time constant 40 will be used in later sections in order to get good performace.

Table III Dimensionless time constant effect (using fixed diode resistance of $R_f = 20^{-1}R_{eng}$ and $R_b = 20R_{eng}$)

Dimensionless Time Constant mcR_{eng}/τ	Scaled Power
40	1
20	1
12.5	0.997
8	0.994
5	0.979
2.1	0.897

3-2-2 Optimization of diode performance.

Second, I fix the time constant and R_{eng} while changing the values of R_f and R_b. In order to eliminate the mass size effect, I chose dimensionless time constant equals to 40. We know that the ideal thermal diode, which has $R_f = 0$ and $R_b = \infty$, should give us the best performance, *the* P_{max}, which is discussed in section 1-2. A thermal diode with very small R_f and very large R_b should give us a performance very close to P_{max}. Fig. 3B demonstrated this. It shows that in general, when the forward resistance gets smaller, the power output gets higher. However, the values of R_b has less effect than R_f. Fig. 3B indicates that when R_b is set to 40 times, 10 times, 5 times and 1 times R_{eng}, the power outputs are almost the same. Only when R_b is smaller than R_{eng}, the significant decrease of power output is observed.

From this chapter, we can conclude that in order to obtain a good performance, I should choose large time constant, very small R_f compared to the R_{eng}, and a reasonably large R_b compare to R_{eng}. Different scenario of thermal diode and thermal capacitor combinations are tested and shown in Table IV. An optimized performance is shown in Fig. 4 with the following parameters as scenario 4 in Table IV(the heat engine assume to be used has thermal resistance 3K/Mand efficiency 5% under hot temperature 230C$_o$ and cold temperature 50C$_o$[13]). In this case, the optimized temperature difference is almost the same as ΔT_{max} and the power is 92.6% of the maximum capability with a ripple 2.6%. P Indicates power.

Table IV Optimized scaling power output under different scenario

Scenario	R_{eng}/R_f	R_b/R_{eng}	mcR_{eng}/τ	$Average\ T_1[K]$	$Average\ T_2[K]$	Scaled Power
1	1000	20	10	356.1	273.7	84.9%
2	1000	10	10	356.1	273.8	84.6%
3	1000	20	40	358.2	271.7	92.8%
4	1000	10	40	358.2	271.7	92.6%

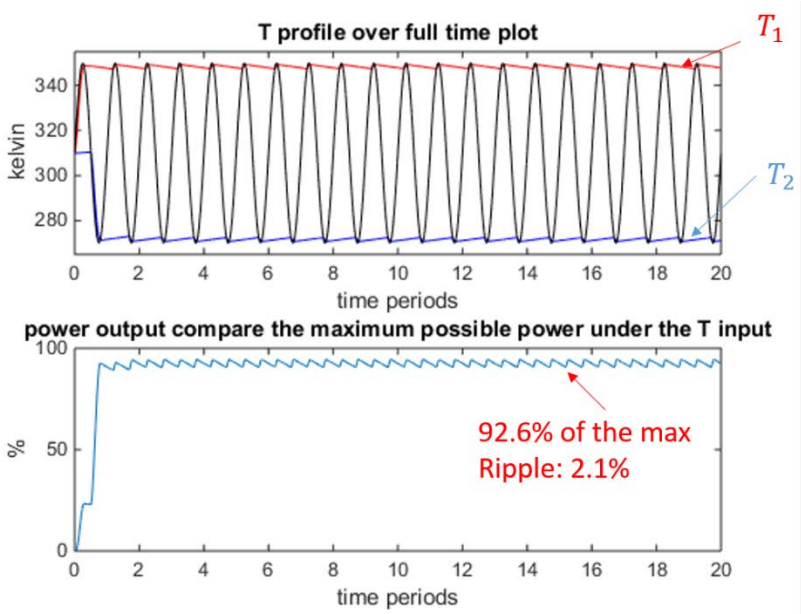

Fig. 4 The optimized performance corresponding to scenario 4 of Table IV. Top: Red line is T_1, blue line is T_2 and black line is the plate temperature T_p. After optimization, we obtained the ΔT very close to ΔT_{max}, which gives us a power output 92.6% out of the maximum possible power (bottom).

3-3. Experimental demonstration

Mitch Westwood in our group designed and led the experiment of testing the thermal diode bridge with temperature boundary condition, as part of a parallel MS project [2]. Fig. 5 shows the comparison of experimental data and the simulation. A commercial thermoelectric heat engine with $\mathrm{P} = 0.08 \times \Delta T^2$(curve fit by M. Westwood[2]) is used. The thermal resistance of the heat engine is 5.8$[KW^{-1}]$, which can be found from the datasheet[14]. A leakage resistance $R_{leak} = 43[KW^{-1}]$ from each mass to ambient is also considered. The temperature boundary condition is a one hour period sinewave with minimum temperature 300K and maximum temperature 350K. The mass size is mc=7600$[JK^{-1}]$ for each mass, providing a dimensionless time constant of 12. From Table III we know that the thermal capacitor effect with dimensionless time constant of 12 is very small. Because of the experimental design limitation, the minimum forward diode resistance we can get is $R_f = \frac{1}{100} R_{eng}$. The backward resistance used in the experiment is $R_b = 20R_{eng}$. From the calculations of Fig.3B, an expected about 65%-70% of maximum power should be obtained.

By using the parameters provided above, the expected temperature profile and power output are shown in Fig. 5C and Fig. 5D. The experimental data is shown in Fig. 5A and Fig. 5B, which give very close results. The power output error between the simulation and the experiment is 7%. However, the actual power output (58.3%) is a little lower than the expected power based on the forward resistance value according to Fig.3B. One reason might be that the time constant used in the experiment is smaller than that used in Fig. 3B. Another possible reason is the leakage effect is added to real case simulation but not included in Fig.3B testing.

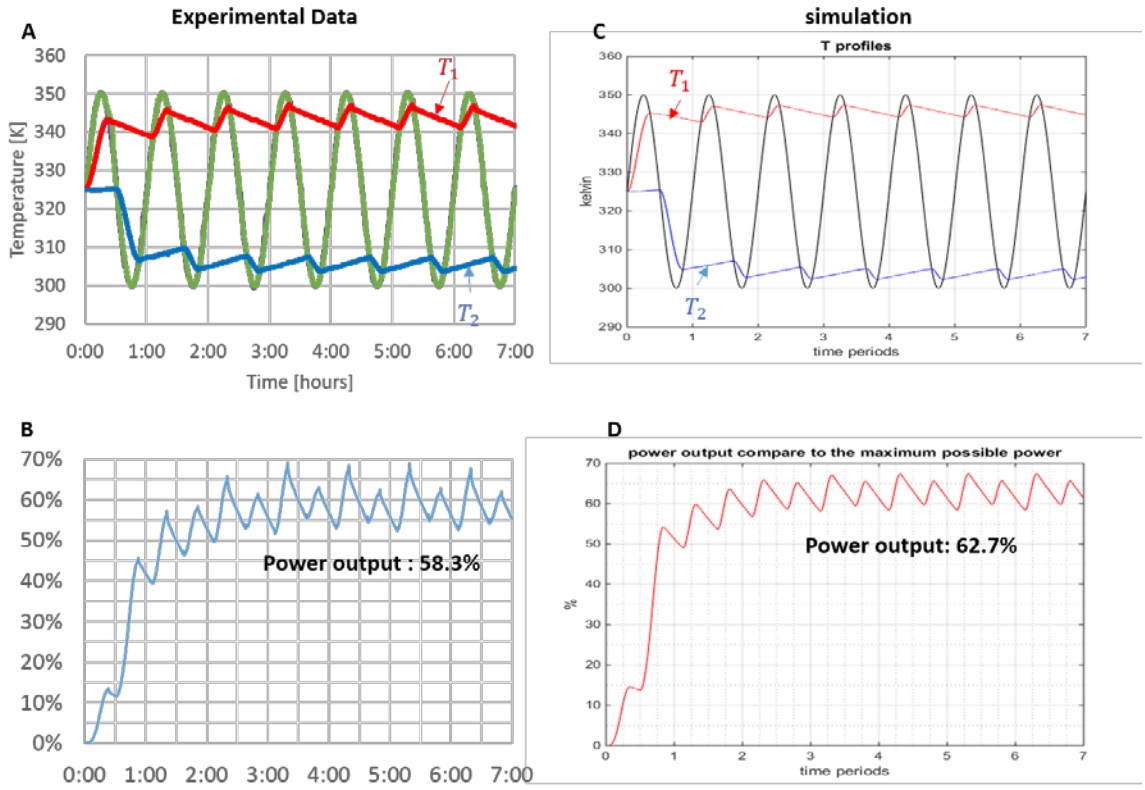

Fig.5 The comparison of the experimental data and the simulation. (A) and (B) are the experimental data while (C) and (D) are simulations. Both temperature profiles and power output from experiment agree with the simulation with an error about 7%.

3-4. Compare to the traditional methods

There are two traditional methods to collect solar heat. One method is to use one thermal switch, which is acting like an active diode, and one mass to store solar thermal energy at the hot side, while use the ground or ambient as a thermal reservoir to provide a constant T_∞ as the cold side. Since the T_∞ is apparently larger than T_2, you can imagine that, with the same type of diode and capacitor, the maximum ΔT can be obtained from this design must be smaller than that from using thermal diode bridge. Based on the fact that the power output is proportional to ΔT^2, and use same power criterion in section 1-2, the difference of the power output will be more significant. Another method, which is a reasonable idea we came up with, is using the blackbody plate as periodic hot and cold source, while using ground or ambient as another thermal reservoir. By using this method, a periodic electrical power wave is obtained and then converted to a relatively constant power by using electrical diode bridge. The maximum power that can be obtained from this system must be periodic and with a maximum value close to the thermal switch method.

The performance of three different systems is shown in Fig. 6. As can be seen, if the T_∞ used in traditional methods equals to the average temperature of the sinewave, the power

output using a thermal diode bridge will be four times larger than using only thermal switch for hot side, and about eight times larger than not using diode or mass. In addition, as can be seen in Fig.6B, the ripple of not using any diode or mass will be 100% by our definition in section 1-2.

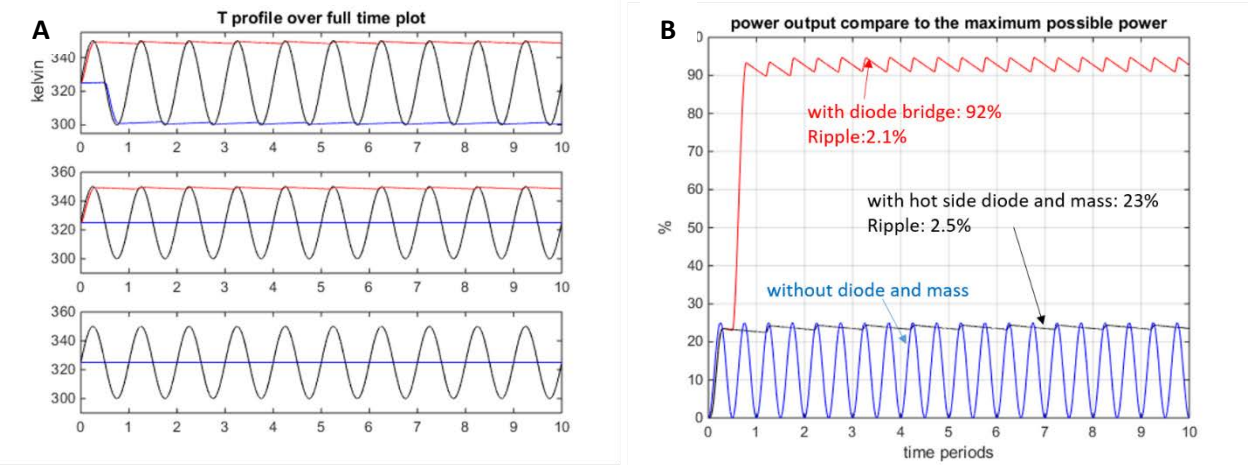

Fig. 6 Temperature profiles and power outputs of three different methods. The temperature profile of hot side and cold side on the top of Fig 6A is the method using the thermal diode bridge. The one in the middle is the method using a diode and a mass on hot side, but using constant T_{avg} as cold side. The one at the bottom is the method using only blackbody plate as one temperature and constant T_{avg} as another temperature. (B) shows the power performance under three different methods, using a thermal diode bridge outputs 92% power which is four times more than 23% which is the power output by using only one thermal switch for hot side, and eight times more than 13% which is the average power of not using any diode or mass.

Chapter 4. Heat flux boundary condition

To evaluate the performance of the thermal diode bridge applied to solar energy collection, heat flux boundary condition is more realistic than temperature boundary condition. From section 2-2, the solar power received on the horizontal surface for a mostly clear day is approximately a half sine wave. Once the boundary condition of the blackbody plate is decided, the temperature of the blackbody plate can be solved. To get the temperature profiles of mass 1 and mass 2, equation (2a) and equation (2b) still apply. The T_p becomes unknown but can be solved from the energy balance equation (4) of the black body plate,

$$q_{solar}(t) - 0.7\sigma(T_p^4 - T_{atm}^4) - 0.3\sigma(T_p^4 - T_{\cos}^4) - h(T_p - T_{amb}) - q_{cond}(t) = 0 \qquad (4)$$

Notice that q_{solar} now is a time dependent variety, and is set to a sine wave input during day time and zero during night time,

$$q_{solar} = \begin{cases} 1000\sin\omega t & \omega t \in (0,\pi) \\ 0 & \omega t \in (\pi, 2\pi) \end{cases}$$

The q_{cond} here is the total conduction between plate and masses, which is the summation of $q_1$and q_2 as shown in Fig.1.

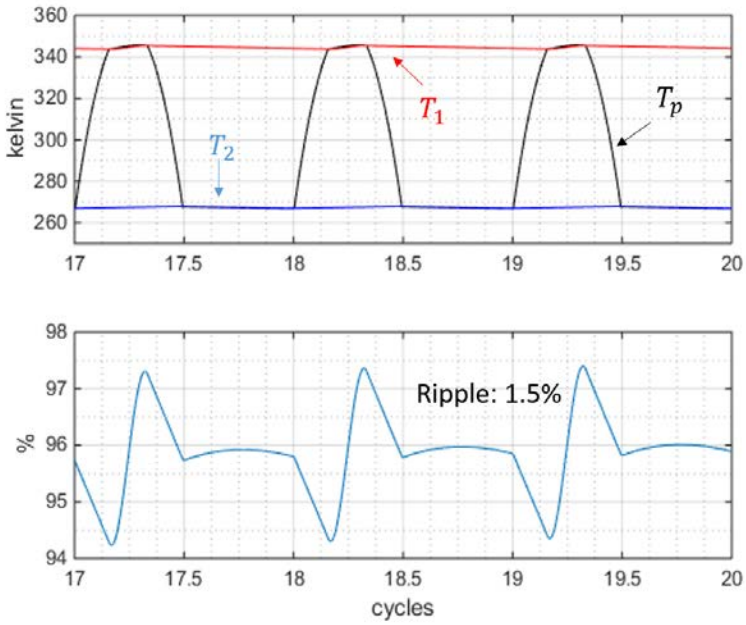

Fig 7 Performance of using the same optimized parameters (scenario 4 of Table IV) of thermal capacitor and thermal diode from temperature boundary condition chapter. The plate temperatureT_p is no longer a sinewave. The conduction from the plate to the diode during charging time pulls down the plate temperature. This conduction effect makes temperature of the two massesT_1 and T_2 more smooth and the ripple smaller. The scaled power in system is about 96%.

Chapter 5. Conclusion and Discussion

5-1 Conclusion

In summary, we have demonstrated both theoretically and experimentally the possibility to use a thermal diode bridge for continuous solar energy harvesting. Based on our modeling results, the thermal mass and the diode are the keys for efficient thermal diode bridges. First, for the thermal mass, ideally we prefer it as large as possible; in reality, we should also consider the cost. To balance between these two concerns, our model suggests a thumb rule: a dimensionless time constant 10 is economically sufficient. Second, for the thermal diode, if the cost is based on the rectifying coefficient (R_b/R_f), we would prefer both forward and backward resistances to be small. For example, with same rectifying coefficient$R_b/R_f = 10^4$, diode which has $R_b = 10R_{eng}$ with $R_f = 10^{-3}R_{eng}$ is better than a diode which has $R_b = 10^2R_{eng}$ with $R_f = 10^{-2}R_{eng}$. However, the so called small R_b here is expected to be larger than R_{eng}. Satisfying these criteria, a thermal diode bridge can improve the power performance of a heat engine by a factor of four, as compared to a traditional scheme.

5-2 Future work

The reason of using half bridge (with two diodes) rather than full bridge (with four diodes) to harvest solar energy is because we don't have another comparable sinusoidal heat source. If we can reach the other side of the earth, making a full thermal diode bridge is possible. The

technology now is not able to achieve that. However, if we have a small object, for example the satellite, making a full thermal diode bridge becomes easier. Fig. 8A is the schematic configuration of a full thermal diode bridge for solar energy harvesting. With an extra heat source oscillating 180^{o}out of phase, a smaller mass provides same performance as half bridge is expected. By using the same parameters from scenario 4 in Table IV, about 95.4% scaled power is achieved. If we want the same power output as shown in Fig.4, we only need dimensionless time constant about 12.

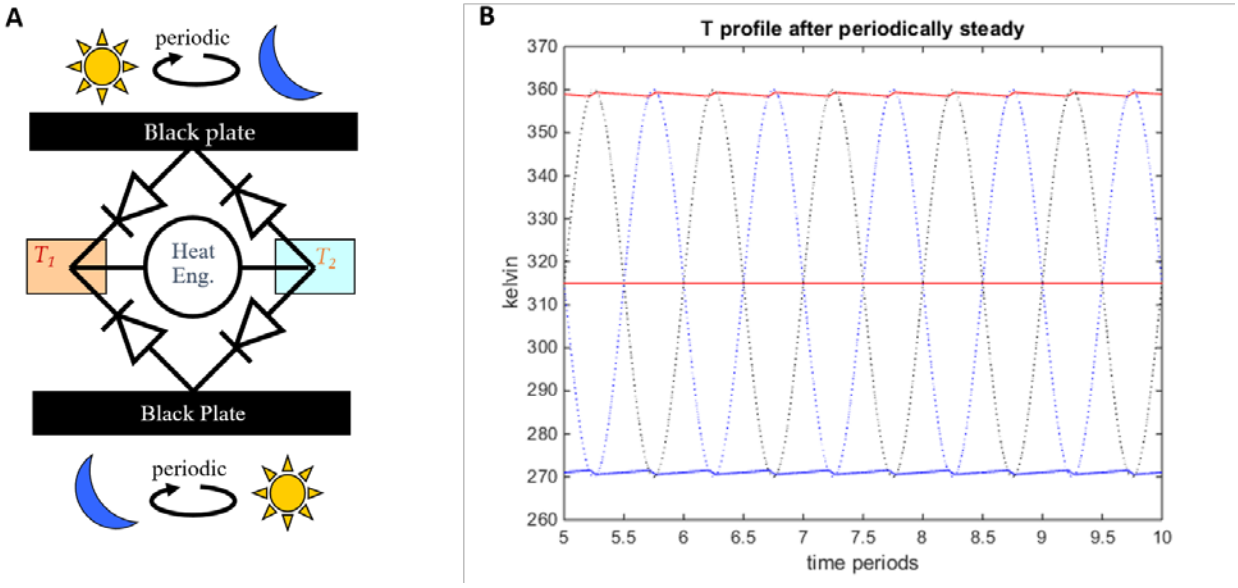

Fig. 8 Configuration of a full thermal diode bridge and its performance. (A) is the structure of the full bridge. Two more diodes are added to connect to another blackbody plate, which provides another heat source with half phase difference than the original plate. (B) is the temperature profile of the two masses by using the full bridge. Upper red line is T_1 and blue line is T_2. The black dotted line the upside plate temperature and blue dotted line the down side plate temperature. Visually a more smooth temperature profiles can be observed.

References

[1] A. R. Hambley, *Electrical engineering: principles and applications*, 5th ed. Pearson, 2009.

[2] M. Westwood, “Thermal Rectification to Increase Power and Efficiency of Solar-Thermal Electricity Generation,” 2015.

[3] Ocallagh.Pw, S. D. Probert, and A. Jones, “a Thermal Rectifier,” *J. Phys. D-Applied Phys.*, vol. 3, no. 9, p. 1352–&, 1970.

[4] C. Dames, “Solid-State Thermal Rectification With Existing Bulk Materials,” *J. Heat Transfer*, vol. 131, no. 6, p. 061301, 2009.

[5] Z. Chen, C. Wong, S. Lubner, S. Yee, J. Miller, W. Jang, C. Hardin, A. Fong, J. E. Garay, and C. Dames, “A photon thermal diode,” *Nat. Commun.*, vol. 5, no. May, p. 5446, 2014.

[6] City of Chicago Department of Environment, “Green Roof Test Plot: 2003 End Of Year Project Summary Report,” no. February, 2004.

[7] M. P. Thekaekara, “Solar radiation measurement: techniques and instrumentation,” *Sol. Energy*, vol. 18, pp. 309–325, 1976.

[8] W. B. Stine and R. W. Harrigan, *Solar Energy: Fundamentals and Design*. John Wiley & Sons, Inc., 1985.

[9] “Berkeley Weather Averages,” *US Climate*, 2015. [Online]. Available: http://www.usclimatedata.com/climate/berkeley/california/united-states/usca0087/2015/1.

[10] D. Andrews, *An introduction to atmospheric physics*, Second. Cambridge University Press, 2010.

[11] S. Catalanotti, V. Cuomo, G. Piro, D. Ruggi, V. Silvestrini, and G. Troise, “The radiative cooling of selective surfaces,” *Sol. Energy*, vol. 17, no. 2, pp. 83–89, 1975.

[12] T. L. Bergman, A. S. Lavine, F. P. Incropera, and D. P. Dewitt, *Fundamentals of Heat and Mass Transfer. 7th Edition*. 2011.

[13] “Thermoelectric Generator (TEG) Modules.” [Online]. Available: http://www.marlow.com/power-generators/standard-generators.html.

[14] T. Modules, “Thermoelectric Modules,” *Ceramics*, pp. 11–12.